ISSN 0021-3640, JETP Letters, 2024, Vol. 120, No. 1, pp. 46–49. © The Author(s), 2024. This article is an open access publication.
Russian Text © The Author(s), 2024, published in Pis'ma v Zhurnal Eksperimental'noi i Teoreticheskoi Fiziki, 2024, Vol. 120, No. 1, pp. 45–48.

CONDENSED MATTER

Interrelation between Doping Dependencies of the Spin Susceptibility and Electronic Structure in Cuprates

V. I. Kuz'min[a,*], M. M. Korshunov[a], S. V. Nikolaev[a,b], T. M. Ovchinnikova[c], and S. G. Ovchinnikov[a,b]

[a] *Kirensky Institute of Physics, Federal Research Center KSC, Siberian Branch, Russian Academy of Sciences, Krasnoyarsk, 660036 Russia*

[b] *Siberian Federal University, Krasnoyarsk, 660041 Russia*

[c] *Sukachev Institute of Forest, Federal Research Center KSC, Siberian Branch, Russian Academy of Sciences, Krasnoyarsk, 660036 Russia*

*****e-mail: kuz@iph.krasn.ru*

Received June 3, 2024; revised June 3, 2024; accepted June 5, 2024

We calculate electronic structure and spin susceptibility dependencies on doping within the framework of a cluster perturbation theory for strongly correlated electronic systems. The change in the susceptibility with increasing doping is qualitatively consistent with the experimental data on resonant inelastic X-ray scattering and inelastic neutron scattering, as well as with the results of the calculations within the quantum Monte Carlo method.

DOI: 10.1134/S0021364024601945

1. INTRODUCTION

Progress in the development of the resonant inelastic X-ray scattering (RIXS) allowed to experimentally obtain information on dynamical magnetic susceptibility [1–3] complementing the results of the inelastic neutron scattering (INS) [4–6]. For cuprates like $La_{2-x}Sr_xCuO_4$, a strong dependence of electronic and magnetic properties on doping x is well known. With increasing x, the system evolves from an antiferromagnetic Mott–Hubbard insulator at $x = 0$ through a still not well understood pseudogap state with the short-range magnetic order to a normal Fermi-liquid-like metal at high dopings $x \propto 0.25$. It is known that the strong electronic correlations (SEC) in cuprates prevent description of their physical properties within the framework of the standard one-electron approximations in a wide region of the phase diagram. To adequately describe the pseudogap state, it is necessary to take into account doping-dependent changes in the short-range antiferromagnetic order. To solve the problem, numerically exact methods for finite clusters are widely used, for example, the quantum Monte Carlo method (QMC) [7–9]. At the same time, translational invariance is also important for both the electronic structure and the collective excitations in a crystal and it can be considered using approaches such as the dynamic mean field theory and its generalizations [10] and within the framework of cluster theories [11]. Here we use cluster perturbation theory (CPT) [12–14] in which the eigenstates of a small cluster are calculated exactly and then used to write the intercluster hoppings and interactions within the framework of the perturbation theory using cluster's eigenstates.

2. CALCULATION METHOD

The method for calculating the electronic structure in CPT is described in many publications and, de facto, is already standard [12–14]. Recently, methods for calculating dynamical charge and spin correlation functions based on CPT were developed [15] and called Charge-CPT and Spin-CPT, respectively. There, exact diagonalization of the 3 × 3 clusters within the Emery model was used. In such a cluster, spin correlations up to the fifth coordination sphere are taken into account exactly. The calculation method is close to the approaches used in [16–18]. In this work, the Spin-CPT is applied to the Hubbard model

$$H = \sum_{i,\sigma}\left\{(\varepsilon - \mu)\, n_{i,\sigma} + \frac{U}{2} n_{i,\sigma} n_{i,\bar{\sigma}}\right\} - \sum_{ij,\sigma} t_{ij} c^{\dagger}_{i,\sigma} c_{j,\sigma}, \quad (1)$$

where $c_{i,\sigma}$ denotes an annihilation operator at the site i with the spin σ, $\bar{\sigma} = -\sigma$, $n_{i\sigma} = c^{\dagger}_{i\sigma} c_{i\sigma}$ is the particle number operator, t_{ij} is the hopping integral, and U is the on-site Coulomb repulsion.

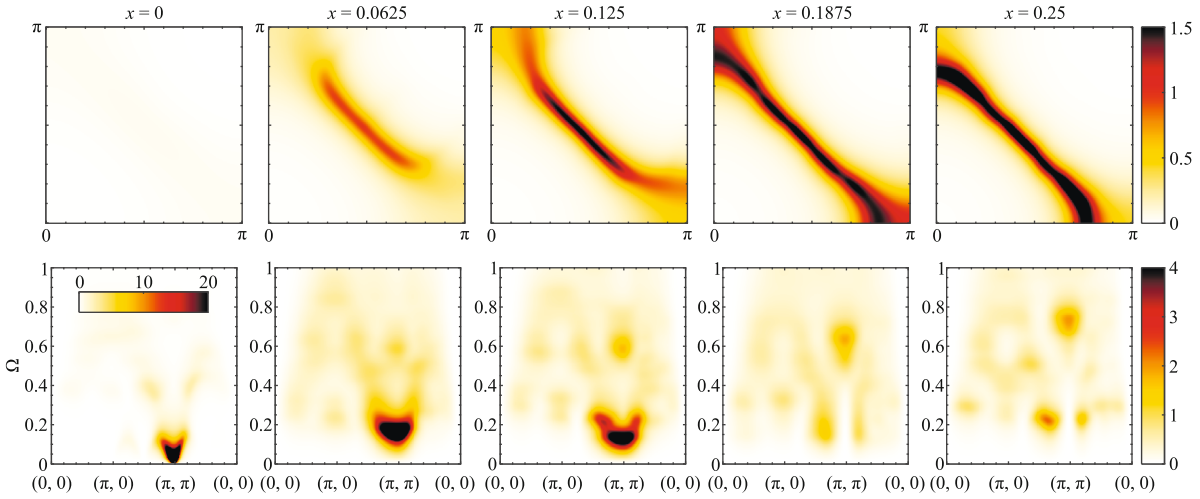

Fig. 1. (Color online) Changes with doping of the spectral density at the Fermi level, essentially, the Fermi surface (top row), and the maps of the spin response $\mathrm{Im}\,\chi(\mathbf{k},\Omega)$ (bottom row) for five doping concentrations, $x = 0$, 0.0625, 0.125, 0.1875, 0.25. Note that for the clarity, the intensity scale in the lower left figure differs from all other figures of the bottom row.

As the first step, the local spin correlation function is calculated exactly in terms of the many-electron eigenstates of the cluster,

$$[\hat{\chi}_c]_{i,j}(\Omega) = \sum_{\mu}\left[\frac{\langle 0|S_i^+|\mu\rangle\langle\mu|S_j^-|0\rangle}{\Omega - (E_\mu - E_0) + i\delta} - \frac{\langle 0|S_j^-|\mu\rangle\langle\mu|S_i^+|0\rangle}{\Omega + (E_\mu - E_0) + i\delta}\right], \quad (2)$$

where indices i and j enumerate cluster sites, $S_i^{+(-)}$ is a spin raising (lowering) operator at site i, $|\mu\rangle$ are the eigenstates of a cluster with energies E_μ, and Ω denotes frequency. The procedure for obtaining the matrix of intercluster interactions is similar to constructing a single-particle CPT on the Hubbard X-operators [14] and leads to a two-particle Green's function in the CPT approximation in a form similar to random phase approximation (RPA):

$$\hat{\chi}_{CPT}^{-1}(\mathbf{k},\Omega) = \hat{\chi}_c^{-1}(\Omega) - \hat{\mathbf{J}}(\mathbf{k}), \quad (3)$$

where $\mathbf{k}$ is the wave vector, the matrix $\hat{\mathbf{J}}(\mathbf{k})$ is obtained by considering intercluster interactions in the limit of the $t - J$ model and is analogous in its structure to the usual hopping matrix $\hat{\mathbf{T}}(\mathbf{k})$ in CPT. The translational invariance of the lattice is restored by calculating the function

$$\chi(\mathbf{k},\Omega) = \frac{1}{N_c}\sum_{i,j} e^{-i(\mathbf{r}_i - \mathbf{r}_j)\mathbf{k}}[\hat{\chi}_{CPT}]_{i,j}(\mathbf{k},\Omega), \quad (4)$$

where $\mathbf{r}_i$ is a position of the site i within a cluster. In this work, we calculate the electronic structure and spin correlation functions using the 4 × 4 cluster that allows us to take into account the short-range magnetic order up to the ninth neighbor exactly.

3. CALCULATION RESULTS

Figure 1 shows the changes with doping in the electronic structure and spin susceptibility within the Hubbard model considering hopping between first and second neighbors with parameters $t = 0.56$ and $t' = -0.06$ and Hubbard repulsion $U = 3.22$. Here and below, the energy is given in eV, and the parameters are selected to reproduce the low-energy electronic structure of the Emery model for cuprates [19]. The top row shows the maps of the electron spectral density distribution at zero frequency, $A(\mathbf{k},\omega = 0)$, in the first quarter of the Brillouin zone. The distribution corresponds to the Fermi surface. In the undoped case of a Mott–Hubbard insulator, the spectral density is vanishingly small everywhere. At low doping $x = 0.0625$, the spectral weight is small for all wave vectors in the antinodal direction, while in the nodal direction there is a maximum of the spectral distribution function; it is the pseudogap state and the widely discussed Fermi arc observed in experiments. For $x = 0.125$, the spectral weight of electrons on the Fermi surface in the antinodal direction is still noticeably lower than in the nodal direction. This state can be called a weak pseudogap with the center of the Fermi surface at the (π, π) point. Near optimal doping $x = 0.1875$, the spectral weight is almost the same over the entire Fermi surface, which is characteristic of a normal Fermi liquid. The distribution of the spectral weight of electrons for the overdoped case $p = 0.25$ indicates that a Lifshitz transition has occurred and a new Fermi

surface has been formed with the center at the $\Gamma = (0,0)$ point.

Let us now analyze the spin susceptibility as a function of the wave vector and the energy (bottom row in Fig. 1). In the undoped case, the spin-wave nature of the excitations is evident with a linear dispersion law and a maximum of the spin response at the (π, π) point. A similar dispersion and distribution of the spectral weight were obtained by the QMC method in [16]. With doping and weakening of the antiferromagnetic correlations, in the vicinity of the (π, π) point, the maximum of the spin response shifts to higher energies. Similar behavior was also obtained by the QMC method [16]. An increase in the energy of spin excitations upon doping was discovered experimentally in the RIXS spectra [18]. These experiments did not reveal the low-energy spin excitations predicted in RPA calculations [20]. Note that at high doping, characterized by the dispersion of almost free electrons ($x = 0.1875$ and $x = 0.25$), the low-energy spin response is present at incommensurate wave vectors that is consistent with the INS data on $La_{2-x}Sr_xCuO_4$ [21, 5], as well as with RPA [20] and the cluster calculations generalization of RPA–CPT-RPA [15].

4. CONCLUSIONS

We studied the evolution of the electronic structure and spin excitations with doping within the cluster perturbation theory for the Hubbard model of cuprates within the 4×4 cluster. We augmented the calculation of the dynamical spin susceptibility based on the cluster perturbation theory within the framework of the Spin-CPT method by the intercluster interaction that has a structure similar to RPA. It is shown how, during the transition from an insulator state to a pseudogap state, a transition from magnon to paramagnon dispersion occurs with a dominant contribution of the spectral weight at the antiferromagnetic wave vector (π, π). At the same time, during the transition from the pseudogap state to a weakly correlated metal, the spin response at low energies is redistributed to incommensurate vectors.

Here we have not observed incommensurate response at low dopings at low energies, which was discovered in $La_{2-x}Sr_xCuO_4$ and YBa_2CuO_{6+x} [4, 5] and obtained within the framework of perturbation theory for strongly correlated electrons [22–25]. In our theory, for the electronic structure characteristic of the pseudogap phase, there is a maximum of spin response at the (π, π) point and excitations are similar to paramagnons. This kind of picture of spin susceptibility was observed in $HgBa_2CuO_{4+\delta}$ [6]. It is possible that other sets of parameters may lead to an incommensurate response such as the lower branch of the "hourglass." It is of interest for further research.

FUNDING

V.I. Kuz'min, S.V. Nikolaev, and S.G. Ovchinnikov acknowledge the support of the Russian Science Foundation, project no. 24-12-00044.

CONFLICT OF INTEREST

The authors of this work declare that they have no conflicts of interest.

REFERENCES

1. L. J. P. Ament, M. van Veenendaal, T. P. Devereaux, J. P. Hill, and J. van den Brink, Rev. Mod. Phys. **83**, 705 (2011).
2. Y. Peng, G. Dellea, M. Minola, et al., Nat. Phys. **13**, 1201 (2017).
3. H. C. Robarts, M. García-Fernández, J. Li, A. Nag, A. C. Walters, N. E. Headings, S. M. Hayden, and K.-J. Zhou, Phys. Rev. B **103**, 224427 (2021).
4. V. Hinkov, P. Bourges, S. Pailhes, Y. Sidis, A. Ivanov, C. D. Frost, T. G. Perring, C. T. Lin, D. P. Chen, and B. Keimer, Nat. Phys. **3**, 780 (2007).
5. O. J. Lipscombe, B. Vignolle, T. G. Perring, C. D. Frost, and S. M. Hayden, Phys. Rev. Lett. **102**, 167002 (2009).
6. M. K. Chan, C. J. Dorow, L. Mangin-Thro, Y. Tang, Y. Ge, M. J. Veit, G. Yu, X. Zhao, A. D. Christianson, J. T. Park, Y. Sidis, P. Steffens, D. L. Abernathy, P. Bourges, and M. Greven, Nat. Commun. **7**, 10819 (2016).
7. N. Prokof'ev, B. Svistunov, and I. Tupitsyn, JETP Lett. **64**, 911 (1996).
8. V. Kashurnikov and A. Krasavin, J. Exp. Theor. Phys. **105**, 69 (2007).
9. E. Gull, A. J. Millis, A. I. Lichtenstein, A. N. Rubtsov, M. Troyer, and P. Werner, Rev. Mod. Phys. **83**, 349 (2011).
10. G. Rohringer, H. Hafermann, A. Toschi, A. A. Katanin, A. E. Antipov, M. I. Katsnelson, A. I. Lichtenstein, A. N. Rubtsov, and K. Held, Rev. Mod. Phys. **90**, 025003 (2018).

11. T. Maier, M. Jarrell, T. Pruschke, and M. H. Hettler, Rev. Mod. Phys. **77**, 1027 (2005).
12. D. Sén'hal, D. Perez, and M. Pioro-Ladrière, Phys. Rev. Lett. **84**, 522 (2000).
13. S. V. Nikolaev and S. G. Ovchinnikov, J. Exp. Theor. Phys. **114**, 118 (2012).
14. V. I. Kuz'min, M. A. Visotin, S. V. Nikolaev, and S. G. Ovchinnikov, Phys. Rev. B **101**, 115141 (2020).
15. V. I. Kuz'min, S. V. Nikolaev, M. M. Korshunov, and S. G. Ovchinnikov, Materials **16**, 4640 (2023).
16. Y. F. Kung, C. Bazin, K. Wohlfeld, Y. Wang, C.-C. Chen, C. J. Jia, S. Johnston, B. Moritz, F. Mila, and T. P. Devereaux, Phys. Rev. B **96**, 195106 (2017).
17. E. M. Pärschke, Y. Wang, B. Moritz, T. P. Devereaux, C.-C. Chen, and K. Wohlfeld, Phys. Rev. B **99**, 205102 (2019).
18. Y. Y. Peng, E. W. Huang, R. Fumagalli, M. Minola, Y. Wang, X. Sun, Y. Ding, K. Kummer, X. J. Zhou, N. B. Brookes, B. Moritz, L. Braicovich, T. P. Devereaux, and G. Ghiringhelli, Phys. Rev. B **98**, 144507 (2018).
19. M. M. Korshunov, V. A. Gavrichkov, S. G. Ovchinnikov, I. A. Nekrasov, Z. V. Pchelkina, and V. I. Anisimov, Phys. Rev. B **72**, 165104 (2005).
20. C. Monney, T. Schmitt, C. E. Matt, J. Mesot, V. N. Strocov, O. J. Lipscombe, S. M. Hayden, and J. Chang, Phys. Rev. B **93**, 075103 (2016).
21. S. Wakimoto, K. Yamada, J. M. Tranquada, C. D. Frost, R. J. Birgeneau, and H. Zhang, Phys. Rev. Lett. **98**, 247003 (2007).
22. M. V. Eremin, A. A. Aleev, and I. M. Eremin, JETP Lett. **84**, 167 (2006).
23. M. V. Eremin, A. A. Aleev, and I. M. Eremin, JETP **106**, 752 (2008).
24. M. V. Eremin, I. M. Shigapov, and I. M. Eremin, Eur. Phys. J. **85**, 1 (2012).
25. M. V. Eremin, I. M. Shigapov, and H. T. D. Thuy, J. Phys.: Condens. Matter **25**, 345701 (2013).

Translated by the authors